Chalcogenide Letters Vol. 9, No. 5, May 2012, p. 185 - 191

FABRICATION AND CHARACTERIZATION OF CIGS SOLAR CELLS WITH In_2S_3 BUFFER LAYER DEPOSITED BY PVD TECHNIQUE

MOHAMMAD ISTIAQUE HOSSAIN[a*]
[a]*Department of Physics*
Univerisiti Brunei Darussalam, Gadong BE 1410, Negara Brunei Darussalam

By virtue of the explosive growth of solar cells, Indium Sulphide is a prominent buffer layer to be used as an alternative to a CdS layer in solar cells. Moreover, it does not contain any toxic material and can lead to produce nontoxic thin film solar cells with excellent optical properties. In this paper, In_2S_3 thin films were deposited onto a CIGS layer using a thermal evaporation technique, at a height of 7.5 cm from target boat to substrate holder. Indium (In) and sulphur (S) powders were evaporated with different In/S ratio to find out the optimum electrical performance. A promising result can be achieved with an efficiency of 2.88 % (with V_{oc} = 0.5136 V, J_{sc} = 30.83 mA/cm^2 and fill factor = 47.65 %) by using CIGS/ In_2S_3 structure with various composition ratio of In and S (In:S=15:6). The various composition of In_xS_y was found to influence the electrical performance. The films were structurally and optically characterized by IV measurement, X-ray diffraction, atomic force microscopy, and scanning electron microscope and UV measurements. From the fabrication results, numerous influences of In_2S_3 buffer layer are investigated which can lead to the fabrication of high efficiency CIGS solar cells.

(Received February 21, 2012; Accepted May 10, 2012)

Keywords: In_xS_y; CIGS, thermal evaporation; MBE, XRD; AFM; SEM

1. Introduction

In_2S_3 allows for a higher short-circuit current (J_{sc}) and, under certain conditions, also a higher open-circuit voltage (V_{oc}). The small difference in the efficiency allows considering In_2S_3 as a good candidate for CdS substitution. Thickness of the buffer is most determinant in giving a rise to a decrease in FF and increase in V_{oc}. On the other hand, J_{sc} parameter shows different behaviour. For a buffer deposited with higher In_2S_3 proportion, the increase in J_{sc} with thickness must be attributed to its contribution to the photocurrent. In this case, In_2S_3, an n-type semiconductor with 2.2 eV energy gap, is forming a real p–n junction device with p-$CuInS_2$, where minority carriers may also be photogenerated.Indium sulphide has become very promising as a buffer layer due to its latent use in solar cells fabrication. It is an III-VI semiconductor material which has prominent application in optoelectronic, photovoltaic industries and photoelectrochemical solar cell devices [1]. In_2S_3 thin films are much stable and possess higher bandgaps (2-2.8eV) which assist these layers in use as a window/buffer layer in In_xS_y/CIGS solar cells [2]. These distinctive properties play important roles in providing the best conversion efficiency in CIGS solar cells. Another important characteristic is that the bandgap of indium sulphide can be increased up to 3.0 eV due to doping of sodium (5%) [6]. It is generally accepted that in highly efficient solar cells the absorber surface is electronically strongly inverted with respect to the p-type bulk CIGS. In CIGS cells with a CdS-buffer, an increasing Cu-depletion of the CIGS surface due to the formation of a Cu-deficient surface defect layer up to the extremal $Cu(In,Ga)_3Se_5$-phase increases the potential barrier for holes by 0.2 eV. Cu diffusion across the CIGS/In_xS_y interface may affect the electrical properties of the In_xS_y/CIGS junction significantly; indeed, the favourable Cu-depletion of the CIGS surface was observed with ALD-grown In_xS_y-

*Corresponding author: shakil_iiuc@yahoo.com

buffers. However, no Cu diffusion was found for the best-performing as-grown cells with compound-evaporated In_xS_y-buffers; however, the effect of annealing on Cu-diffusion in these cells is still under investigation. Air- and vacuum-annealing of the complete cells result in an improvement of the band gap. Without doubt, post annealing also leads to a redistribution of elements and thus to a (partial) removal of structural and chemical instabilities of the buffer layer or the In_xS_y-interfaces [8]. For ALD–In_2S_3, an optimal deposition and annealing temperature of about 210 to 220°C is well established. On the other hand, for a thinner In_2S_3 layer the absorption edge is in the 400-500 nm while for CdS it is in 500-550 nm [8]. The films can be prepared with different deposition techniques and each technique shows exclusive results in terms of optical characteristics. These various methods are chemical bath deposition (CBD) with a bandgap of 2.0-2.8 eV [1], thermal evaporation technique (2-2.3 eV, 2.8 eV) [2], physical vapor deposition (2.46-2.73 eV), ALCVD (2.7 eV) [7], ultrasonically sprayed (2.0-2.8 eV) sputtering technique (2.4 eV) [8]. In this paper, the composition ratio of In/S was varied and various effects in the InS and CIGS interface have been found. Among all these methods, PVD/thermal evaporation has shown favorable results due to its simplicity, simple operation process, and low deposition amperage, which results in low cost, easy production of large area and research applications. As the deposition current is less, the temperature of evaporation is comparatively lower which helps to give a low defect density. From the interface study (Fig. 1) it can be explained that at the interface of In_xS_y/CIGS, there are fewer defect states. This occurs due to the fewer lattice constant mismatch of indium sulphide and CIGS and this will result in higher photocurrent. In addition, a spike in the conduction band is eliminated due to the suitable combination of electron affinities and doping level [9].

2. Experimental procedures

Soda lime glass (SLG) is used as the substrate for CIGS solar cell. SLG is cut into small pieces measuring 1.5 cm x 2.5 cm. The thickness of the SLG is typically around 3 mm. A Molybdenum (Mo) back contact was deposited by sputtering process. The thickness of Mo sputtered is 0.7 µm. CIGS polycrystalline thin film absorber layer was deposited by using molecular beam epitaxy (MBE) co-evaporation technique. The Mo/SLG samples were mounted on the substrate holder and transferred into the deposition chamber. Deposition chamber is vacuumed until the base pressure reaches 10^{-9} Pa. One of the advantages of using MBE is that it has the capability of achieving ultra high vacuum in its deposition chamber which minimizes contamination on the samples during the deposition process. Substrates are baked at 550 °C to remove any impurities and to thermally activate the Mo surface layer prior to the CIGS deposition. There are 4 effusion cells (also known as Knudsen cells or K-cells) that contain high purity elemental copper (Cu), selenium (Se), gallium (Ga) and Indium (In) in it. These effusion cells are heated at various temperatures to produce elemental beam fluxes that are directed towards the substrate holder and the beam fluxes are monitored by 4 individual beam flux monitor. The operating pressure during the deposition process is around 4 x 10^{-6} Pa. The initial beam fluxes of the elements are blocked by the shutters in front of the K-cell for 5 – 10 minutes as it might contain impurities. In_xS_y was evaporated by Ulvac Kiko VPC- 060 thermal apparatus on top of CIGS samples. The purity of In and S powder was 99.999% to prepare the various composition ratios of In_xS_y. After preparing the composition of In and S, it was placed in the tungsten boat. A vacuum pressure of $4x10^{-3}$ pa was used to evaporate the target and evacuation time was 20 minutes. The distance from boat to substrate holder was 7.5 cm. In addition, we noted the In_xS_y was completely evaporated. The films were characterized by an X-ray diffractometer in the scanning range of 10-60°(2θ). The surface morphology images were obtained by atomic force microscopy, grain sizes were captured by SEM.

Table (1) Composition ratio used in fabrication.

	Composition	Height (target to substrate) cm	In powder (gm/mol)	S powder (gm/mol)	Evaporation current(amp)/ time (min)
Sample 1	In_xS_y	7.5	0.093	0.0384	25/5
Sample 2	In_xS_y	7.5	0.186	0.0768	28/6
Sample 3	In_xS_y	7.5	0.1395	0.0576	30/5
Sample 4	In_xS_y	7.5	0.279	0.1152	32/5

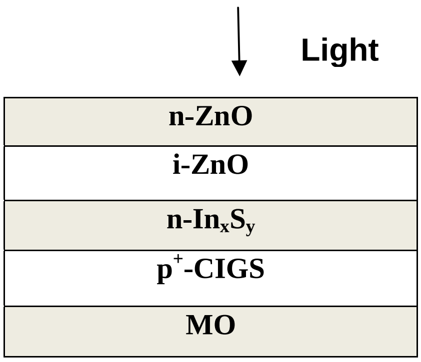

Fig. 1: The structure of CIGS solar cell with In_xS_y buffer layer used in fabrication

3. Results and discussions

The study of the layers using XRD & SEM revealed the presence of In and S. This different ratio of In and S shows very impressive result in terms of crystallinity, homogeneity, and bandgap. The average percentage of indium ratio in the layers is 70%.

3.1 XRD Analysis

The structural analysis of indium sulphide thin films was evaluated by an X-ray diffractometer with different diffraction angle 2θ from 10° to 60°. Figure 2 show the XRD pattern for In_2S_3 as deposited and annealed at 100 ^oC, 200 ^oC deposited by the thermal evaporation technique. Peaks in different orientations such as (100), (400), (0012), (311) etc exhibit the InS polycrystalline growth. Focusing on one prominent orientation like In_2S_3 (400), one can easily find out the lattice parameter deviation. For sample 1 (In:S=5:2) after annealing at 200^oC a strong peak of β-In_2S_3 (400) phase has been revealed. From the XRD pattern of sample 4 (Figure 2) it can be illustrated that after annealing at 100 ^oC and 200 ^oC In_2S_3 has the same preferential (0012) orientation. So from here it can be explained that film crystallinity is affected by the deposition environment, annealing temperature and also by the composition ratio of the materials. With higher temperature, the atoms will gain sufficient energy to be reoriented and will be much more stable with better crystallinity. However, before deposition there are many amorphous crystallites present and this exhibit less intense peaks. After annealing at a particular temperature better crystallinity are observed. These changes may be attributed to the coalescence induced grain growth during the annealing process where smaller nuclei can easily rotate compare to the larger nuclei in order to minimize the interfacial energy [3].

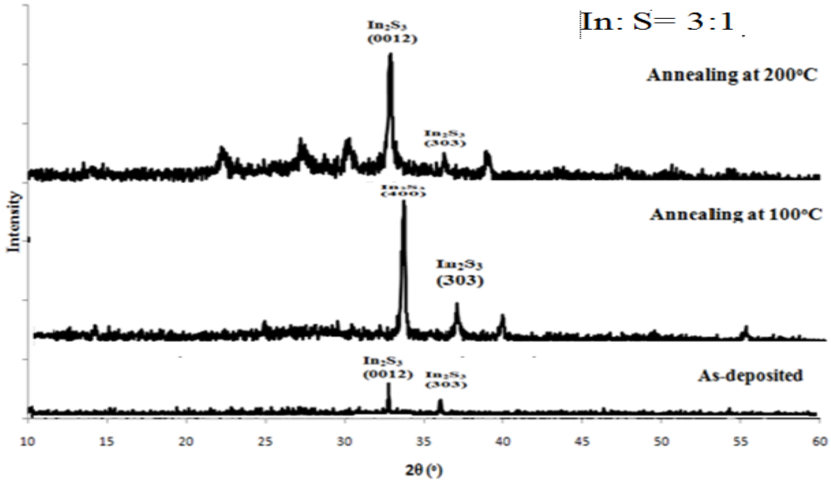

Fig. 2. X-ray diffraction patterns of sample 4 (In/S= (0.279/0.1152)gm/mol

Fig. 3 below shows the XRD result of the fabricated CIGS absorber layer.

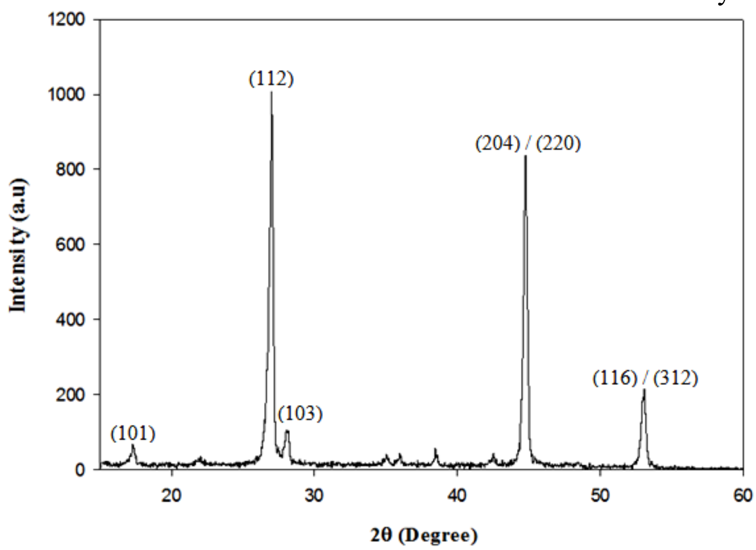

Fig. 3: XRD plot for CIGS thin film layer with Miller indices(s) for each peak

It can be clearly seen that there are 3 major peaks that represent 3 different crystal orientations in the film. The highest peak is centred exactly at 27 º which corresponds to (112) preferred orientation. The second highest peak is centred at 44.8 º which corresponds to (204) / (220) crystal orientation and the third highest peak is centred at 53.12º corresponding to (116) / (312) crystal orientation. Two other minor peaks are also detected at 17.32º and 28.04 º also corresponding to CIGS crystals with (101) and (103) orientations. The secondary phase of Cu_xSe which has XRD reflection at several different 2θ angles was not detected indicating high quality absorber layer was grown. Sintered compound of Cu_xSe is conductive and can cause shunting if it comes to contact with the Mo back contact. A residue of Cu_xSe secondary phase usually exists on the layer surface due to excess Cu and Se evaporation during the second stage. Hence, non-existence of Cu_xSe phase implies the Cu and Se evaporated in the second stage is consumed during the third stage in order to make the film overall Cu-poor.

3.2 Surface Morphology Study by SEM

Scanning electron microscope images for sample 4 (In:S=15:6) with different compositions at various temperatures are shown in figure 4. These figures illustrate the nice full coverage of the films with less pinholes. From the figures it can be determined that a polycrystalline material with larger grain boundaries will have less interface states which act as recombination centers. The results showed that roughness was increasing with the layer thickness. If grain boundary is larger than the diffusion length less carriers will recombine.

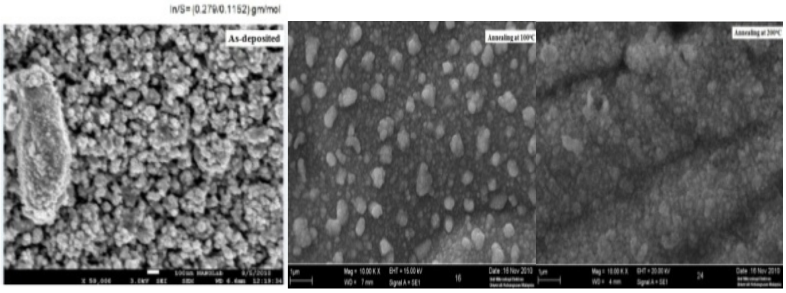

Fig. 4: SEM images of sample 4 (In/S= (0.279/0.1152)gm/mol (In:S=3:1).

Fig. 5 below shows the surface and cross sectional view of CIGS film observed with SEM. SEM results show very good coverage on top of Mo.

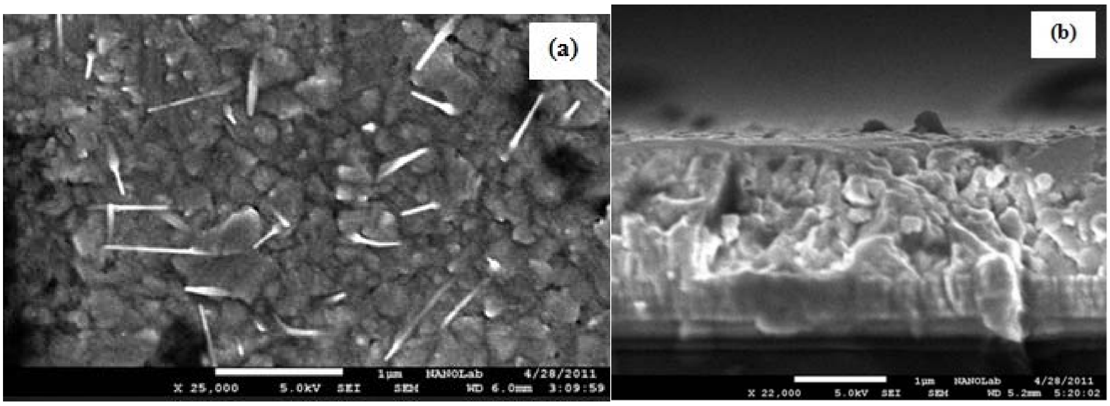

Fig 5: SEM results for CIGS film. (a) Surface morphology. (b) Cross section.

Fig. 6 shows the cross sectional view for the whole structure where it can be seen that the In_xS_y layer is evenly deposited on top of the CIGS absorber layer.

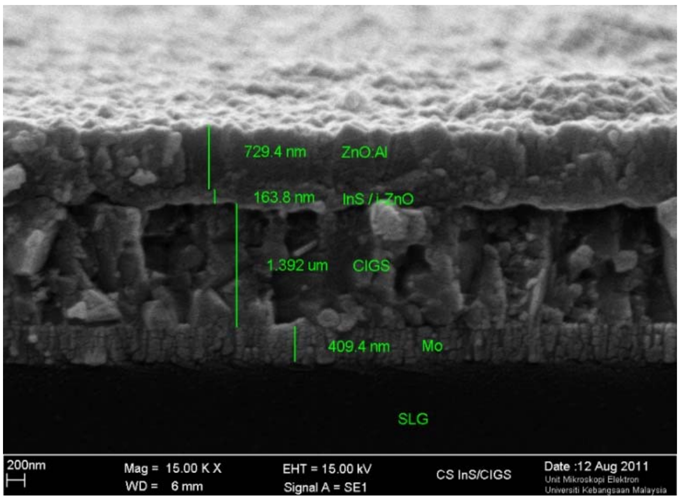

Fig. 6 SEM results for CIGS solar cell (Cross Section)

3.4 Optical Characterization of Indium Sulphide Layer

The optical properties were studied with UV-spectroscopy.

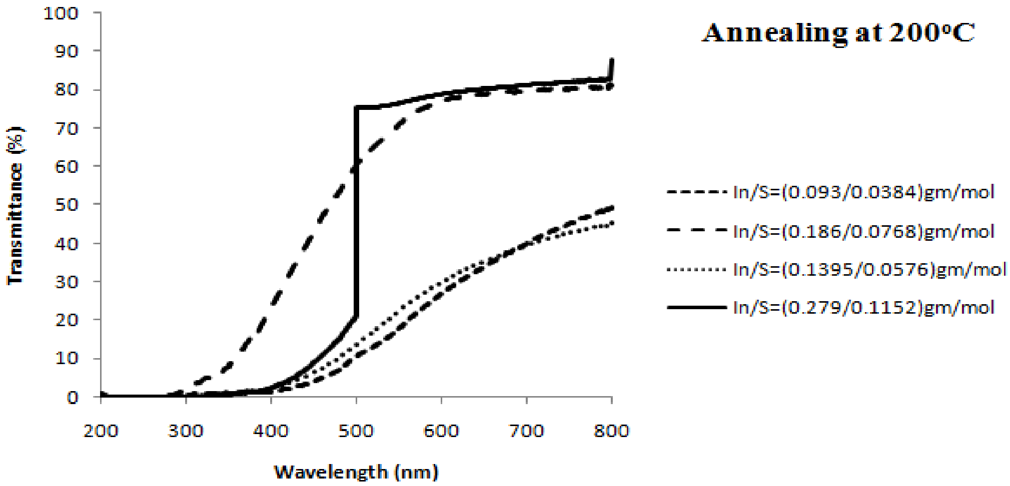

Fig. 7: Transmittance (%) vs. Wavelength (nm), annealing at 200°C

After deposition, for sample 4 (Figure 7) with the composition ratio of In/S= (0.279/.1152) gm/mol has transmission of 80 % in 400-500 nm regions because of less absorption of light in the layer. Due to less absorption of photon in this layer, it can be used as a buffer layer so that most of the photons will be absorbed by the absorber layer. From our fabrication results, the bandgap was found to be in range from 2.3 to 2.5 eV for the as deposited samples. The extrapolation of straight line portion of the plot to the zero absorption coefficients gives the bandgap energy. Generally in polycrystalline semiconductors, the bandgap can be affected by the stoichiometric deviation, quantum size effect and disorder at grain boundaries [3]. Lower bandgaps for the as deposited samples can be related with the structural disorder and result in defect states in the forbidden energy gap. In addition, if the room temperature increases rapidly, it will effect in lower bandgap. The thermal vibration which happens due to higher temperature, acts to reduce the bandgap energy. Moreover, the bandgap variation can be related with the variation of particle size. Therefore, the possibilities of developing the films in terms of bandgap can be attributed to the composition ratio of indium sulphide, particle size and deposition temperature.

3.5 IV Characterization of Solar Cell

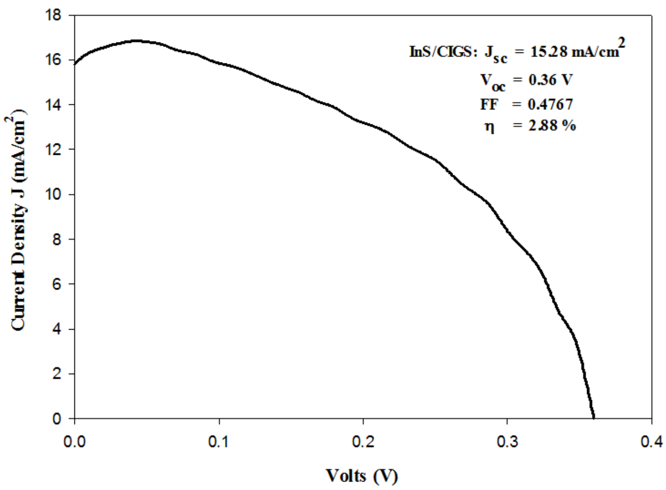

Fig. 9: I-V characteristics of cells with InS (In:S = 15:6) buffer layer .

Open circuit voltage (Voc) and short circuit current density (Jsc) of the CIGS solar cells are also shown in Figure 9. Electron-hole pair (EHP) generation is the major factor, which happens for the collection of longer wavelength of lights in the absorber layer. Therefore, the value for Voc and Jsc are increase. It is also investigated that for In_2S_3 phase where S> 60% at lower percentage of S, InS or In_6S_7 will be produced. For $In_2S_{(3+x)}$ the best electrical performances can be achieved [6]. In addition, fill factor (FF) increases with the thinner In_2S_3 layer, which can be related to the no band discontinuity or spikes at the valance band interfaces. However, low Voc and Jsc can occur due to recombination at the CIGS absorber layer when an electron (or hole) is trapped by an energy state in the forbidden region which is introduced through defects. Therefore, fewer electrons will contribute to the quantum efficiency of the solar cell and the value for Voc and Jsc will be low.

4. Conclusions

Thermally evaporated In_xS_y films with different composition ratios have been studied. From the XRD analysis it has been investigated that the samples have β-In_2S_3 structure with (400) and (311) planes as the preferred orientation. The optical bandgaps for the samples were found from 2.1-3.05 eV which has been improved by controlling the ratio of materials during deposition. From this practical analysis of hetero-structure solar cells with In_2S_3, the electrical performances for the CIGS solar cells have been investigated in terms of buffer layer material composition ratio. The composition ratio of In and S played an important role to achieve the better electrical performance. In_2S_3 shows very promising results as an alternative choice of a toxic CdS buffer layer. A new challenge to fabricate large-area p-CIGS/ n-In_2S_3 thin film photovoltaic has been opened up by using the new device structure.

Acknowledgement

The author would like to acknowledge Dr. Martin Blundell for his invaluable contribution to all ongoing thin film photovoltaic research at the Universiti Brunei Darussalam.

References

[1] Puspitasari, T.P. Gujar, K.D. Jung, O.S. Journal of Materials Processing Technology **201,** 775–779 (2008).
[2] Timoumi,A., Bouzouita, H., Kanzari, M. & Rezig, B. Journal of Thin Solid Films **480–481**, 124–128 (2005).
[3] Revathi, N. Prathap, P. Miles, R.W. & Ramakrishna Reddy, K.T. Annealing effect on the physical properties of evaporated In_2S_3 films. Journal of Solar Energy Materials & Solar Cells. 2010
[4] Lokhande, C.D. Ennoui, A. Patil, P.S., Giersig, M. K., Diesner, M. & Muller, H.. Journal of Thin Solid Films pp. 18-23. 1999
[5] Ras, A.D., Kostorz, G., Hariskos, D. Menner, R., Powalla, M.S., Tiwari, N.A. Journal of Thin Solid Films **517**, 2792 (2009).
[6] Spiering,S., Hariskos,D., Powalla, M., Naghavi, N. & Lincot,D.. Journal of Thin Solid Films **431–432**, 359 (2003).
[7] Spiering , S., Eicke, A., Hariskos, D., Powalla , M. Naghavi, N., Lincot, D. Journal of Thin Solid Films **451 –452**, 562–566 (2004).
[8] Ernits, K., Brémaud, D., Buecheler, S., Hibberd, C.J., Kaelin, M. Khrypunov, G. Müller, U, Mellikov, E. & Tiwari, A.N.. Characterisation of ultrasonically sprayed In_xS_y buffer layers for Cu(In,Ga)Se_2 solar cells. Journal of Thin Solid Films **515**, 6051 (2007).
[9] Green, M.A. 1982. Solar Cells Operating Principles, Technology, and System Applications. New Jersey: Patience-Hall, Inc.